



Published in final edited form as:

*Immunity*. 2015 April 21; 42(4): 665–678. doi:10.1016/j.immuni.2015.03.011.

## C-Myb<sup>+</sup> Erythro-Myeloid Progenitor-Derived Fetal Monocytes Give Rise to Adult Tissue-Resident Macrophages

Guillaume Hoeffel<sup>1</sup>, Jinmiao Chen<sup>1</sup>, Yonit Lavin<sup>2,3</sup>, Donovan Low<sup>1</sup>, Francisca F. Almeida<sup>1</sup>, Peter See<sup>1</sup>, Anna E. Beaudin<sup>4</sup>, Josephine Lum<sup>1</sup>, Ivy Low<sup>1</sup>, E. Camilla Forsberg<sup>4</sup>, Michael Poidinger<sup>1</sup>, Francesca Zolezzi<sup>1</sup>, Anis Larbi<sup>1</sup>, Lai Guan Ng<sup>1</sup>, Jerry K.Y. Chan<sup>1,5,6,7</sup>, Melanie Greter<sup>8</sup>, Burkhard Becher<sup>8</sup>, Igor M. Samokhvalov<sup>9</sup>, Miriam Merad<sup>2,3</sup>, and Florent Ginhoux<sup>1,\*</sup>

<sup>1</sup>Singapore Immunology Network (SiGN), Agency for Science, Technology and Research (A\*STAR), 8A Biomedical Grove, IMMUNOS Building #3-4, BIOPOLIS, 138648 Singapore

<sup>2</sup>Department of Oncological Sciences, The Tisch Cancer Institute, 1425 Madison Avenue, New York, NY 10029, USA <sup>3</sup>The Immunology Institute, Icahn school of Medicine at Mount Sinai, 1425 Madison Avenue, New York, NY 10029, USA <sup>4</sup>Institute for the Biology of Stem Cells, Department of Biomolecular Engineering, University of California-Santa Cruz, 1156 High Street, Santa Cruz, CA 95064, USA <sup>5</sup>Experimental Fetal Medicine Group, NUHS Tower Block level 12, Yong Loo Lin School of Medicine, National University of Singapore, 1E Kent Ridge Road, 119228 Singapore

<sup>6</sup>Reproductive Medicine, KK Women's and Children's Hospital, 100 Bukit Timah Road, 229899 Singapore <sup>7</sup>Singapore and Cancer and Stem Cell Biology Program, Duke-NUS Graduate Medical School, 8 College Road, 169857 Singapore <sup>8</sup>Institute of Experimental Immunology, University of Zürich, Winterthurerstrasse 190, CH-8057 Zürich, Switzerland <sup>9</sup>Guangzhou Institutes of Biomedicine and Health, Chinese Academy of Science, 190 Kai Yuan Avenue, Science Park, Guangzhou, 510530 China

<sup>6</sup>Reproductive Medicine, KK Women's and Children's Hospital, 100 Bukit Timah Road, 229899 Singapore <sup>7</sup>Singapore and Cancer and Stem Cell Biology Program, Duke-NUS Graduate Medical School, 8 College Road, 169857 Singapore <sup>8</sup>Institute of Experimental Immunology, University of Zürich, Winterthurerstrasse 190, CH-8057 Zürich, Switzerland <sup>9</sup>Guangzhou Institutes of Biomedicine and Health, Chinese Academy of Science, 190 Kai Yuan Avenue, Science Park, Guangzhou, 510530 China

<sup>6</sup>Reproductive Medicine, KK Women's and Children's Hospital, 100 Bukit Timah Road, 229899 Singapore <sup>7</sup>Singapore and Cancer and Stem Cell Biology Program, Duke-NUS Graduate Medical School, 8 College Road, 169857 Singapore <sup>8</sup>Institute of Experimental Immunology, University of Zürich, Winterthurerstrasse 190, CH-8057 Zürich, Switzerland <sup>9</sup>Guangzhou Institutes of Biomedicine and Health, Chinese Academy of Science, 190 Kai Yuan Avenue, Science Park, Guangzhou, 510530 China

<sup>6</sup>Reproductive Medicine, KK Women's and Children's Hospital, 100 Bukit Timah Road, 229899 Singapore <sup>7</sup>Singapore and Cancer and Stem Cell Biology Program, Duke-NUS Graduate Medical School, 8 College Road, 169857 Singapore <sup>8</sup>Institute of Experimental Immunology, University of Zürich, Winterthurerstrasse 190, CH-8057 Zürich, Switzerland <sup>9</sup>Guangzhou Institutes of Biomedicine and Health, Chinese Academy of Science, 190 Kai Yuan Avenue, Science Park, Guangzhou, 510530 China

<sup>6</sup>Reproductive Medicine, KK Women's and Children's Hospital, 100 Bukit Timah Road, 229899 Singapore <sup>7</sup>Singapore and Cancer and Stem Cell Biology Program, Duke-NUS Graduate Medical School, 8 College Road, 169857 Singapore <sup>8</sup>Institute of Experimental Immunology, University of Zürich, Winterthurerstrasse 190, CH-8057 Zürich, Switzerland <sup>9</sup>Guangzhou Institutes of Biomedicine and Health, Chinese Academy of Science, 190 Kai Yuan Avenue, Science Park, Guangzhou, 510530 China

### Summary

Although classified as hematopoietic cells, tissue- resident macrophages (MFs) arise from embryonic precursors that seed the tissues prior to birth to generate a self-renewing population, which is maintained independently of adult hematopoiesis. Here we reveal the identity of these embryonic precursors using an in utero MF-depletion strategy and fate-mapping of yolk sac (YS) and fetal liver (FL) hematopoiesis. We show that YS MFs are the main precursors of microglia, while most other MFs derive from fetal monocytes (MOs). Both YS MFs and fetal MOs arise from erythro-myeloid progenitors (EMPs) generated in the YS. In the YS, EMPs gave rise to MFs without monocytic intermediates, while EMP seeding the FL upon the establishment of blood

\*Correspondence: florent\_ginhoux@immunol.a-star.edu.sg.

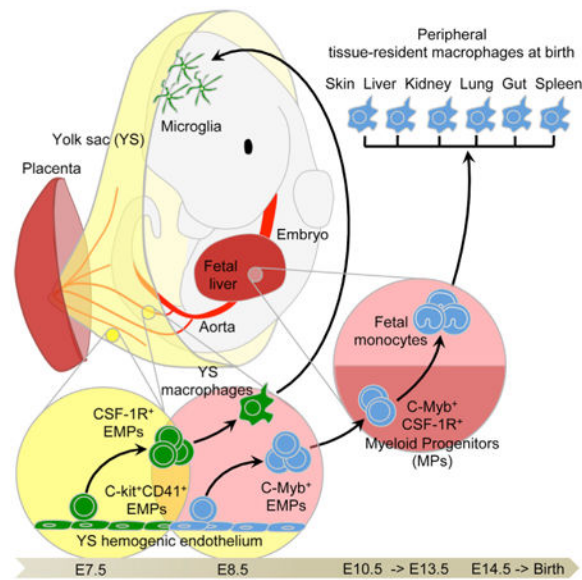
**Author Contributions:** F.G. and G.H. conceived the study; G.H., Y.L., D.L., F.F.A., P.S., A.E.B., J.L., I.L., and M.G. performed experiments; G.H., Y.L., A.E.B., E.C.F., and M.G. analyzed data; G.H., J.C., M.P., F.Z., and F.G. analyzed bioinformatics data; L.G.N., A.L., J.K.Y.C., and I.M.S. provided reagents; B.B., I.M.S., and M.M. provided intellectual guidance; and F.G., M.M., and G.H. wrote the paper.

**Accession Numbers:** The microarray data are available in the Gene Expression Omnibus (GEO) database <http://www.ncbi.nlm.nih.gov/gds> under the accession number GSE66970.

Supplemental Information: Supplemental Information includes five figures, three tables, and Supplemental Experimental Procedures and can be found with this article online at <http://dx.doi.org/10.1016/j.immuni.2015.03.011>.

circulation acquired c-Myb expression and gave rise to fetal MOs that then seeded embryonic tissues and differentiated into MFs. Thus, adult tissue- resident MFs established from hematopoietic stem cell-independent embryonic precursors arise from two distinct developmental programs.

## Graphical abstract



## Introduction

Macrophages (MFs) are mononuclear phagocytes with crucial roles in development, tissue homeostasis, and the induction of immunity. However, they can also contribute to the pathological processes of tumor growth and metastasis, as well as chronic inflammatory diseases including atherosclerosis and diabetes (Lavin and Merad, 2013). There is growing interest in the clinical manipulation of MF populations, but realizing their therapeutic potential will require improved knowledge of their origins and the mechanisms underlying their homeostasis.

Since the definition of the mononuclear phagocyte system (MPS) (van Furth et al., 1972), the prevailing dogma has stated that tissue-resident MF populations are replenished by monocytes (MOs) from the blood. While this proves true for dermal and gut MFs (Bain et al., 2014; Tamoutounour et al., 2013), MOs do not substantially contribute to many adult tissue MF populations either in the steady state, or even during inflammation (Hashimoto et al., 2013; Jakubzick et al., 2013; Jenkins et al., 2011; Yona et al., 2013); rather, the majority of tissue-resident MF populations are established during development by embryonic precursors and maintain themselves in adults by self-renewal (Epelman et al., 2014; Ginhoux et al., 2010; Guillems et al., 2013; Hoeffel et al., 2012; Schneider et al., 2014; Schulz et al., 2012). Despite these advances in knowledge, the nature and origin of the embryonic precursors of MFs remain unknown.

Several spatially and temporally regulated waves of hematopoietic cells are produced in mammalian embryos, culminating with the establishment of hematopoietic stem cells (HSCs) in the bone marrow (BM) (Orkin and Zon, 2008; Tavian and Pèault, 2005). In mice, the first hematopoietic progenitors appear in the extra-embryonic yolk sac (YS), around embryonic age 7.0 (E7.0), where they initiate primitive hematopoiesis, producing mainly nucleated erythrocytes and MFs (Moore and Metcalf, 1970). From E8.25, multi-lineage erythro-myeloid progenitors (EMPs) and lympho-myeloid progenitors (LMPs) emerge in the YS as a “second wave,” termed the transient definitive stage (Frame et al., 2013; Lin et al., 2014; Palis et al., 1999). EMPs are also found in other hemogenic tissues such as the placenta and umbilical cord (Dzierzak and Speck, 2008) and enter the circulation to colonize the fetal liver (FL) from E9.5 (Lin et al., 2014). After E8.5, the intra-embryonic mesoderm commits to the hematopoietic lineage and new waves of hematopoietic progenitors emerge: first in the para-aortic splanchnopleura (P-Sp) region and then in the aorta, gonads, and mesonephros (AGM) region (Lin et al., 2014). The hematopoietic activities of the P-Sp and AGM regions generate the pre-HSC and mature HSC that colonize the FL around E10.5 (Kieusseian et al., 2012; Kumaravelu et al., 2002) to finally establish definitive hematopoiesis (Golub and Cumano, 2013; Medvinsky et al., 2011; Orkin and Zon, 2008). The FL becomes the major hematopoietic organ after E11.5, generating all hematopoietic lineages and expanding the definitive HSC population before their migration to the spleen and the BM (Christensen et al., 2004).

YS MFs first appear within the YS blood islands at E9.0 in both mouse and rat, and develop without passing through a monocytic intermediate stage (Takahashi et al., 1989). They are the primary source of microglia, the resident MFs of the central nervous system (Ginhoux et al., 2010), and also give rise to a minor fraction of Langerhans cells (LCs), the specialized antigen-presenting cells of the skin (Hoeffel et al., 2012). The major fraction of adult LCs derives from fetal MOs generated in the FL from E12.5 and recruited into fetal skin around E14.5 (Hoeffel et al., 2012). Fetal MOs also contribute to populations of adult MFs in lung alveoli (Guilliams et al., 2013; Schneider et al., 2014) and in the heart (Epelman et al., 2014). Using fate-mapping to distinguish cells arising from primitive versus definitive hematopoiesis initially suggested that adult MF populations in lung, dermis, and spleen arise predominantly from definitive hematopoiesis with negligible contribution from YS MFs (Ginhoux et al., 2010). However, a new approach exploiting the differential dependence of MFs on the transcription factor *c-Myb* has since indicated that *c-Myb*-independent YS MFs may be the sole origin of MFs in the lung, liver, and pancreas, as well as of microglia and LCs (Schulz et al., 2012). Hence, the embryonic route of origin of tissue-resident MF populations in the adult remains controversial. Our understanding is further hampered by not knowing whether fetal MOs actually arise from definitive HSC or HSC-independent progenitors such as LMPs or EMPs.

We combined *in vivo* YS MF depletion with several fate-mapping models of YS MFs and/or FL MOs to conclusively show that YS MFs are the main precursors of microglia, whereas most other MF populations derive from fetal MOs that seed the tissues around E13.5. Fetal MOs in turn are revealed to derive sequentially from HSC-independent and -dependent routes, the former being the major pathway arising from *c-Myb*<sup>+</sup> EMPs.

## Results

### Tissue-Resident Macrophages Are Seeded Before Birth and Proliferate In Situ

MF embryonic precursors include YS MFs and fetal MOs generated in the FL (Epelman et al., 2014; Guillems et al., 2013; Hoeffel et al., 2012; Schneider et al., 2014). At E10.5, YS MFs (CD45<sup>+</sup> CD11b<sup>lo</sup>F4/80<sup>hi</sup>Ly6C<sup>-</sup>), but not MOs, are present in the YS and throughout the body of the embryo proper (Hoeffel et al., 2012; Naito et al., 1990). At E12.5, YS MFs, but not MOs, were found in liver, skin, kidney, lung, and brain rudiments (Figure 1A). However, as in the developing skin (Hoeffel et al., 2012), an influx of fetal MOs (CD45<sup>+</sup>CD11b<sup>hi</sup>F4/80<sup>lo</sup>Ly6C<sup>+</sup>) was evident at E14.5 in all tissue rudiments tested (Figure 1B, blue population), except the brain (Figures 1B–1D). Fetal MOs appear in the FL around E12.5 (Naito et al., 1990) and exist as two populations differentially expressing Ly6C, similar to adult MOs in the BM (Geissmann et al., 2003). Both populations of fetal MOs also express the chemokine receptor CCR2 (Figure 1C), though it is not required for their emigration from the FL or recruitment into tissues (Figure S1), unlike in their adult counterparts (Serbina and Pamer, 2006). Ly6G<sup>+</sup>CCR2<sup>-</sup> granulocyte progenitors were also detected at E14.5 (Figure S1). In contrast to adult BM MOs, fetal MOs only began to express the chemokine receptor CX3CR1 in the blood, following FL emigration (Figure 1C). Upon tissue infiltration, fetal MOs further upregulated expression of CX3CR1 and the MF markers CD64 and MerTK, and downregulated Ly6C (Figure 1C), suggesting their differentiation into tissue MFs. The early tissue MF populations (Figure 1B–1E, red population) decreased in numbers between E10.5 and E16.5, so that fetal MOs became the major myeloid cell population in the tissues at E16.5 (Figures 1D and 1E). The initial abundant proliferation of both fetal MO sub-populations and MFs within the tissues also gradually diminished with time (Figure 1F, Figure S2). By late embryogenesis, these populations coexisted in every tissue, without presenting any clear signs of apoptosis (Figure S2). Thus, both YS MFs and fetal MOs contribute to tissue MF populations present in the developing embryo.

### YS Macrophages Are Not Required for Fetal Macrophage Development

To understand whether YS MFs were the sole progenitors of MFs in the adult, we asked what impact their in utero depletion would have on the subsequent generation of tissue MFs. The colony-stimulating factor 1 receptor (CSF-1R) is expressed on YS MFs and fetal MOs, but only the development of the former is dependent on CSF-1R (Ginhoux et al., 2010; Hoeffel et al., 2012). Thus, we attempted to deplete YS MFs by transiently inhibiting the CSF-1R signaling pathway with a blocking anti-CSF-1R antibody (clone AFS98), as recently described (Squarzoni et al., 2014). AFS98 injection at E6.5 efficiently depleted MFs in the E10.5 YS (Figure 2A), as well as most embryonic tissue MFs from E10.5 to E14.5 (Figure 2B, red population), but not circulating MOs (Figure 2B, blue population). The depletion of most MFs in AFS98-exposed embryos was transient and receded around E17.5 (Figure 2C, red population). In contrast, embryonic microglia were fully depleted from E10.5 to E14.5, and only partially repopulated at E17.5 (Figures 2A–2C), but fully repopulated after birth (Squarzoni et al., 2014). These data suggest that YS MFs are dispensable for generating tissue-resident MFs in the embryo, and therefore another

CSF-1R-independent embryonic precursor can functionally replace YS MFs during development.

### **Except for Microglia, Only a Minor Fraction of Tissue Macrophages Derives from YS Macrophages**

To define the relative contribution of YS MFs to the tissue MF compartment, we used a fate-mapping mouse model expressing the tamoxifen-inducible Cre recombinase gene (*MerCreMer*) under the control of the CSF-1R promoter (*Csf1r<sup>Cre/WT</sup>*) (Qian et al., 2011). We crossed the *Csf1r<sup>Cre/WT</sup>* mice with the Cre- reporter mouse strain *Rosa26<sup>R26-EYFP/R26-EYFP</sup>* (*Rosa<sup>EYFP</sup>*) and induced recombination in embryos by a single injection of Hydroxytamoxifen (4'OHT) into E8.5 pregnant females. Because CSF-1R is expressed on YS MFs, which appear in the YS from E9.0 (Ginhoux et al., 2010; Hoeffel et al., 2012), this strategy should specifically EYFP-label YS MFs and their progeny. We then measured the relative numbers of EYFP<sup>+</sup> myeloid cells in E8.5 4'OHT-exposed embryos at E13.5 and E16.5, at birth, and in adulthood (Figure 3A). At E13.5, approximately 63.2% ( $\pm 5.6$ ) of MFs in the YS and rudiments of brain, liver, skin, kidney, and lung were EYFP<sup>+</sup>, indicating their common YS MFs origin. From E13.5 onward, the extent of labeling of most MFs declined, reaching 2%–3% at birth, whereas microglia maintained a labeling frequency above 60% throughout adulthood.

To confirm the data from the *Csf1r<sup>Cre/WT</sup>* mice, we used a fate-mapping model possessing a tamoxifen-inducible Cre recombinase gene (*MerCreMer*) under the control of one of the endogenous promoters of the runt-related transcription factor 1 (*Runx1*) locus (Samokhvalov et al., 2007). Because *Runx1* is expressed in hematopoietic progenitors, YS MF or fetal MO progeny could be traced by injecting 4'OHT at E7.5 or E8.5, respectively (Hoeffel et al., 2012). To assess the contribution of YS MFs to myeloid cell populations, we analyzed the frequency of EYFP<sup>+</sup> myeloid cells in embryos and adult mice exposed to 4'OHT at E7.5 (Figure 3B). E13.5 embryos contained similar proportions of labeled MFs in the YS (22.2% $\pm$ 0.9%) and brain rudiment (23.6% $\pm$ 1.1%), suggesting their common origin. However, in liver, lung, skin, and kidney rudiments, significantly fewer fetal MFs were labeled (15.5% $\pm$ 1.3;  $p = 0.002$ ) (Figure 3B). After this time, EYFP labeling decreased to 2%-3% by birth and into adulthood; the same basal amounts as other leucocytes (Ginhoux et al., 2010). These data are consistent with the minor contribution of YS progenitors to the adult HSC pool shown previously (Samokhvalov et al., 2007). In contrast, the microglial population maintained abundant EYFP labeling from E13.5 into adulthood, confirming their YS MF origin (Ginhoux et al., 2010; Hoeffel et al., 2012). Therefore, while YS MFs seed embryonic tissues prior to the emergence of FL hematopoiesis, they do not contribute to adult tissue MF populations, apart from microglia. The absence of apoptosis within the YS MF population in tissues (Figure S2) suggests that the decreasing relative abundance of these cells from E13.5 likely results from dilution by unlabeled immigrant cells.

### **Adult Tissue-Resident Macrophages Derive Predominantly from Fetal Monocytes Generated during Definitive Hematopoiesis**

On the basis of our observations in the skin (Hoeffel et al., 2012), we hypothesized that the fetal MOs infiltrating the tissue rudiments (Figure 1) were the diluting cell population. As

expected, fetal MOs were not labeled in *Csf1r*<sup>Cre/WT</sup> × *Rosa*<sup>EYFP</sup> (*Csf1r*<sup>Cre/EYFP</sup>) embryos activated at E8.5 or in *Runx1*<sup>Cre/WT</sup> × *Rosa*<sup>EYFP</sup> (*Runx1*<sup>Cre/EYFP</sup>) embryos activated at E7.5 (Figure 3C), while injecting 4'OHT into pregnant *Runx1*<sup>Cre/WT</sup> mice at E8.5 is known to mark fetal MOs and their progeny (Hoeffel et al., 2012). Exposure to 4'OHT at E8.5 led to EYFP expression in most tissue MFs in both embryos and adult mice, and not in microglia (Figure 3D). The proportion of EYFP<sup>+</sup> MFs and fetal MOs from E16.5 onward was comparable, suggesting that fetal MOs likely contribute to the EYFP signal observed in tissue MFs (Figure 3E).

To establish whether fetal MOs directly give rise to the tissue MFs that are maintained into adulthood, we devised a Cre-based fate-mapping model to specifically track fetal MOs and their progeny. Following comparative gene-expression analysis in fetal MOs and MFs (Figure 3F and complete list in Figure S3), and confirmation by quantitative RT-PCR (Figure 3G), we based our model on the specific expression of *S100A4* (*FSP1*) in fetal MOs, because this approach has previously been successful in fate-mapping of myeloid cells (Bhowmick et al., 2004; Hashimoto et al., 2013). We then crossed *S100a4*<sup>Cre/WT</sup> mice with the Cre-reporter mouse strain *Rosa*<sup>EYFP</sup> and analyzed the labeling of myeloid cells during development. Fetal MOs exhibited a high labeling frequency (64.5%±6.7) (Figure 3H), whereas E10.5 YS MFs, YS progenitors such as EMPs, and most other leukocytes were labeled far less frequently (17.8%±2.7) (Figure 3I and Figure S3). Therefore, we concluded that *S100a4*<sup>Cre/WT</sup> mice represent a specific fetal MO fate-mapping model, and so proceeded to assess the labeling of tissue-resident MFs (Figure 3I). We hypothesized that MFs derived from fetal MOs should exhibit the same extent of EYFP labeling as fetal MOs. From E14.5 onward, the percentage of EYFP<sup>+</sup> fetal MFs (28.4±3.6%) was markedly greater than the percentage of EYFP<sup>+</sup> YS MFs and microglia (18.6±2.3%) and plateaued at the same extent as that of the fetal MO population (64.5±6.7%; Figures 3H and 3I). This implies that fetal MFs do not arise solely from YS MFs, and that fetal MOs are the dominant source of MFs throughout development. Because EYFP labeling reached a plateau between E17.5 and birth, and remained stable into adulthood (Figure S3), fetal MO-derived MFs must also be capable of maintenance by self-renewal. This is in agreement with newborn BM transplant experiments that showed minor post-natal contribution before 12 weeks after transplantation to adult tissue-resident MFs in the brain, epidermis, liver, kidney, and lung, while dermal, gut, and peritoneal MFs exhibited significant donor origin (Figure S3), likely arising from postnatal blood MO as previously published (Bain et al., 2014; Tamoutounour et al., 2013). Of note, the relative number of EYFP<sup>+</sup> FL MFs was relatively greater than at other sites as early as E12.5, suggesting that fetal MOs differentiate locally into MFs in the FL before moving to other tissues (Figure 3I).

### Fetal Monocytes Derive from HSC -Dependent and -Independent Progenitors

We next investigated the origin of MOs generated in the FL and observed a differentiation continuum of progenitors, as in adult BM (Figure 4A), where MOs derive sequentially from macrophage-dendritic cell precursors (MDPs) and common monocyte progenitors (cMoPs) (Ginhoux and Jung, 2014; Hettinger et al., 2013). We found Lin<sup>-</sup>cKit<sup>+</sup>Flt3<sup>+</sup>CSF-1R<sup>+</sup>Ly6C<sup>-</sup> MDP-like progenitors in the FL (FL MDP) at E12.5-16.5 (Figure 4A and Figure S4) alongside Lin<sup>-</sup>cKit<sup>+</sup>Flt3<sup>-</sup>CSF-1R<sup>+</sup>Ly6C<sup>+/-</sup> myeloid progenitors (MPs), all of which were

highly proliferative (Figure 4B) and exhibited nucleolar structures typical of chromatin reorganization (Figure 4C). The phenotype of the Ly6C<sup>+</sup> MP fraction is equivalent to that of cMoP (Hettinger et al., 2013), whereas the Ly6C<sup>-</sup> fraction of MP is absent in adult BM, and therefore might be a transient embryonic MP population specific to the FL (Figure 4A). We thus named them, FL cMoP and FL MP, respectively.

To clarify the relationships between these progenitors, we isolated them from E14.5 FL and adult BM and compared their gene-expression profiles (GEO GSE66970). Unsupervised clustering analysis revealed the close proximity of each of the FL progenitors to their BM counterparts (Figure 4D), but while fetal MOs selectively expressed genes related to cell cycle and differentiation, adult MOs exhibited an expression profile consistent with their roles in immune responses and pathogen recognition (Figure 4E). We also compared the gene-expression signatures of each progenitor population by Connectivity Map (CMAP) analysis (Figure 4F and Supplemental Methods). This showed that FL MPs and FL MDPs are most closely related; FL cMoP thus, seem to be an intermediate between these two populations and fetal MOs, consistent with their higher proliferative capacity (Figure 4B) and lower expression of *CCR2*, *CX3CR1* and *Lysozyme* (Figure S4) compared to fetal MOs. Upon culture in vitro with CSF-1, both FL MDPs and FL MPs gave rise to MOs through a cMoP stage (Figure S4), as seen in adult BMs (Hettinger et al., 2013). However, the FL MP stage was not detected in FL MDP cultures, suggesting that these two progenitors are independent from each other. Thus, we hypothesized that two pathways of fetal MO generation coexist in the E14.5 FL, perhaps differing in their dependence on HSCs.

To assess the contribution of HSC to fetal MO generation, we examined progenitors and myeloid cells at different fetal stages in mice expressing the Cre-recombinase under the control of the *Flt3* promoter, which labels HSC progeny in adult BM (Boyer et al., 2011). As HSC specification and maintenance are *Flt3*-independent (Boyer et al., 2011; Buza-Vidas et al., 2011), few HSC were labeled at E13.5 (2.17±0.99%) (Figure 4G), while the FL MDP population exhibited steadily increased labeling (from 20% at E13.5, to 67% at E17.5, and 82% at birth) (Figure 4G). Labeling of cMoP, MOs, and MFs at E17.5 was significantly lower than of MDP and remained low throughout (Figure 4G), suggesting a minor contribution from *Flt3*-dependent MDP to fetal MOs and MFs. These data suggest that fetal MOs arise via a *Flt3*-, and perhaps also HSC-, independent pathway.

To distinguish the roles of the two pathways in fetal MO generation, we investigated the lineage potential of FL progenitors. We identified differentially expressed genes in each population (Figure S4) and performed a Gene Set Enrichment Analysis (GSEA) using recently published lineage-associated genes (Böiers et al., 2013; Table S1). A significant enrichment in lymphoid genes expression including *Gata3*, *Rag1*, *Rag2*, and *Il7r* is shown in FL MDP (Figure S4, Table S2), similar to the E9.5 YS lympho-myeloid progenitors (LMPs) that colonize the FL at E11.5 (Böiers et al., 2013). This might indicate some heterogeneity within the fetal MDP population, consisting first of YS-derived LMP during late development and then of bona fide MDP after birth, which are related to those in adult BMs and derive from HSCs. In contrast, FL MPs expressed erythroid- and megakaryocyte-associated genes (Figure S4, Table S2) including as *Klf1*, *Gata1*, and *Itga2b* (CD41), similar

to YS erythro-myeloid progenitors (EMPs), which colonize the FL around E10.0 (Frame et al., 2013): thus FL MPs might derive from EMPs. Finally, FL cMoP and fetal MOs shared an enrichment in myeloid gene expression, whereas lymphocyte, erythrocyte, and megakaryocyte potentials were lost at the cMoP stage, consistent with their monocytic commitment (Figure 4H and Table S2). A heatmap of the genes that were differentially expressed in each progenitor population, based on recently published myeloid-associated genes and transcription factors (Friedman, 2002; Molawi and Sieweke, 2013), highlights the distinction between fetal MDPs and the other fetal myeloid populations (Figure S4), suggesting a closer proximity between FL MPs, FL cMoPs, and fetal MOs and implying that the transient FL MPs, likely the progeny of EMPs, are the main source of fetal MOs.

### **c-Myb<sup>+</sup> EMPs Colonize the Fetal Liver and Generate Fetal Monocytes**

To conclusively define the origin of fetal MOs, we returned to the *Runx1*<sup>Cre/WT</sup> fate-mapping model and asked whether we could label the “transient definitive” wave that generates EMPs in the YS (Palis et al., 1999). We injected 4'OHT either at E7.5, E8.5, or E9.5 and compared the frequency of EYFP<sup>+</sup> FL progenitors, Lin<sup>-</sup>CD48<sup>-</sup>c-Kit<sup>+</sup>Sca-1<sup>+</sup>CD150<sup>+</sup> HSCs, MOs, and MFs at E13.5 (Figure 5A). Injection of 4'OHT at E7.5 exclusively labeled YS MFs in the FL, while injection at E9.5 predominantly led to labeling of HSCs and sequentially decreasing labeling frequencies in FL MDPs, FL MPs, FL cMoPs, fetal MOs, and MFs. Thus, E9.5 injection labels HSC-progeny, and reconfirms the limited involvement of HSCs in the generation of fetal MOs and MFs, as shown in Figure 4. 4'OHT injection at E8.5 led to a high frequency of EYFP<sup>+</sup> FL MPs, FL cMoPs, fetal MOs, and MFs, but labeled only a minor fraction of HSCs, FL MDPs (Figure 5A), and did not label the pre-HSCs, which are generated in the P-Sp/AGM at E9.0 before seeding the FL at E11.0 (Figure S5). More precisely, 4'OHT injection at E8.5 labels YS CD41<sup>+</sup> EMPs (Frame et al., 2013) en route to the FL at E10.0, and their progeny (Figure 5B). Thus, E8.5 injection labels EMPs and their progeny.

Because YS EMPs have been implicated in the generation of YS MFs (Kierdorf et al., 2013), while in our hands they also give rise to fetal MOs once they seed the FL, we decided to investigate their fate in these sites. As expected, EMPs arise before YS MFs, which appear from E9.5 (Figures 5C and 5D and Figure S5), in line with their developmental relationship (Cline and Moore, 1972; Kierdorf et al., 2013). Moreover, MFs were seen in the absence of any monocytic precursors before E12.5 (Figure 1), and as described (Cline and Moore, 1972; Hoeffel et al., 2012; Takahashi et al., 1989). In the *Runx1*<sup>Cre/WT</sup> model, both E7.5 and E8.5 YS EMPs gave rise locally to YS MFs able to migrate to the FL (Figures 5E and 5F), however, E7.5-labeled EMPs remained in the YS and poorly entered the blood circulation, whereas E8.5-labeled EMPs efficiently reached the blood circulation and the FL (Figure 5E, left panel). This suggests that early EMPs differentiate locally, mainly generating YS MFs and erythrocytes before the onset of blood circulation, whereas later EMPs can reach the FL through the blood circulation, as reported (Palis and Yoder, 2001). Of note, E8.5 labeled EMPs that seed the FL still produced MFs locally, but did not substantially contribute to the microglial population at E13.5 (Figure 5E, right panel).

We then followed the fate of late EMPs from the YS to the FL using the *Runx1<sup>Cre/WT</sup>* model, focusing on their E8.5 EYFP<sup>+</sup> progeny (Figures 5F and 5G). EMPs lost the ability to generate MFs with time. From E11.5, intermediate CD11b<sup>hi</sup> F4/80<sup>lo</sup> CSF-1R<sup>+/-</sup> populations emerge, suggesting that EMPs give rise to multiple myeloid progenitors, which in turn generate granulocytes and MOs. MF populations only enlarge again at E16.5 once the fetal MO population is established (Figure 5G). Hence, we hypothesized that the YS *Runx1<sup>+</sup>* hemogenic endothelium initially gives rise to two types of EMPs: early EMPs (labeled at E7.5), which only generate local YS MFs, and late multipotent EMPs (labeled at E8.5) that reach the FL and differentiate into multiple lineages, including MOs that ultimately generate tissue MFs. This is supported by a previous study indicating two waves of phenotypically-similar MF-committed precursors possessing distinct clonal differentiation potentials and arising sequentially in the YS, the first at E8.0 and the second at E8.25 (Bertrand et al., 2005).

We confirmed this hypothesis using the *Csf1r<sup>Cre/WT</sup>* fate-mapping model. 4'OHT injection at E8.5 in the *Csf1r<sup>Cre/WT</sup>* model efficiently labeled EMPs and YS MFs at E10.5 in the YS and the FL (Figure 5H). However, increased decoupling between the tagging frequencies of EMPs and MFs occurred with time, suggesting that early EMPs are not maintained but are instead rapidly replaced by later EMPs. Accordingly, in CSF-1R reporter mice, EMPs did not express CSF-1R on their surface at E9.0 but did express it at the mRNA level (Figure S5), while from E10.0 in the inducible *Csf1r<sup>Cre/WT</sup>* fate-mapping model EMPs were EYFP<sup>-</sup>, explaining why neither late EMPs nor fetal MOs were labeled. In summary, in agreement with our previous data suggesting the presence of two distinct types of EMPs, over time EMPs lose their ability to produce YS MFs but likely become able to give rise to other lineages in the FL, including MOs. As the c-Kit<sup>+</sup> population that contains EMPs was absent in the FL of mice lacking c-Myb (Schulz et al., 2012), expansion and/or differentiation of later EMPs might be regulated by c-Myb expression, as previously suggested (Mucenski et al., 1991). Indeed, c-Myb was expressed in EMPs, LMPs, and cMoPs in the FL, as well as in the YS at E9.5, when EMPs ceased to give rise to YS MFs (Figure 5I). Thus, tissue-resident MFs rely on the generation of fetal MOs from c-Myb<sup>+</sup> EMPs.

## Discussion

Here, we defined the origin and nature of the embryonic progenitors of major adult tissue-resident MF populations. Combining in utero YS MF depletion and fate-mapping models revealed that YS MFs colonize every tissue at mid-gestation, but are dispensable for the generation of all adult tissue-resident MFs. The exception to this was the microglial population of the central nervous system: elsewhere YS MFs were replaced by MFs derived from fetal MOs. By using a fate-mapping model for fetal MOs, we showed that they colonized all embryonic tissues, apart from the brain, and differentiated into tissue MFs able to self-renew into adulthood. We also showed that these fetal MOs arose mostly from YS-derived late EMPs, while YS MFs arose from early EMPs. Thus, although arising from HSC-independent EMPs, fetal tissue MF populations are generated via two distinct developmental programs from two fundamentally different precursors: YS macrophages and FL monocytes.

Our results shed light on fetal monopoiesis, identifying and characterizing the early embryonic progenitors of fetal MOs. Fetal MOs appeared to differentiate through a process related to adult BM monopoiesis, starting from the FL MDP or FL MP that differentiated into FL cMOP intermediates and then Ly6C<sup>+</sup> MOs. Two sources of fetal MOs existed: a first, HSC-independent, wave that arose mostly from YS-derived EMPs and accounted for the majority of fetal MOs present from E12.5–17.5; and a second, HSC-dependent, wave that generated a minor fraction of the fetal MO population after E17.5. In mice expressing the Cre-recombinase under the control of the Flt3 promoter (Boyer et al., 2011), the fetal MDP population was abundantly labeled, indicating their derivation through an Flt3-dependent pathway. However, labeling frequency in fetal MFs did not increase to the same amount as FL MDPs, suggesting a minor contribution to fetal MOs and MFs from the Flt3-dependent pathway. Fetal MDPs exhibited a lymphoid gene-expression signature, consistent with a contribution from LMPs to fetal monopoiesis, though this could not be assessed in the fate-mapping models used. Recent data from a *Rag1*<sup>Cre</sup> fate-mapping model suggested that LMPs are unlikely to contribute to adult myeloid populations (Böiers et al., 2013). However, as only 50% of LMPs express Rag1, their contribution may have been underestimated. Whether the Flt3 lineage-tracing model allows us to unambiguously follow fetal HSC or LMP progeny remains to be formally established.

Primitive hematopoiesis begins within the YS blood islands from E7.0 (Moore and Metcalf, 1970), and is characterized by the emergence of nucleated erythrocytes, hence the denomination “primitive” which relates to the red cells of inferior species such as fish, amphibians, and birds that remain nucleated throughout their lifespan (Palis, 2014). Such denomination was extended to MFs in the YS due to their concomitant development before the emergence of FL hematopoiesis. However, the notion of primitive versus definitive has been rather ambiguous for MFs but could now be clarified by our findings. Here, we have revealed a further layer of complexity to fetal MF generation: using our Runx1 fate-mapping system, we identified an early wave of E7.5 Runx1<sup>+</sup> progenitors that give rise to the EMPs, which differentiate locally into YS MF, and a distinct second later wave of E8.5 Runx1<sup>+</sup> progenitors that give rise to the EMPs, which retain the ability to differentiate locally into YS MFs, or migrate to seed the FL following the establishment of blood circulation from E9.0. The two waves of EMPs differed in their lineage potency and capacity to generate MO intermediates in the FL and YS. MFs deriving in the YS from either early or late EMPs did not seem to go through a monocytic intermediate stage, but rather followed a “fast-track” differentiation pathway, as previously described (Takahashi et al., 1989). Hence, the denomination “primitive macrophage” could now be used to refer to MFs generated in the YS without a monocytic intermediate, and might even be extended to early EMPs that differentiate locally in the YS, to distinguish them from definitive EMPs that give rise to MO intermediates in the FL. Whether early primitive EMPs and late definitive EMPs represent two heterogeneous progenitors arising from independent sources or rather a single population arising from a shared hematopoietic wave of progenitors and exists along a continuum of maturation stages in response to external stimuli, requires clarification. However, it is tempting to speculate that the contrasts in differentiation potential do not reside in the intrinsic potential given by their ontogeny, but rather in the extrinsic signals provided by the local environment. In fact, their multi-lineage potential is revealed upon

establishment of blood circulation, which allows late YS EMPs to access the FLs where they encounter a microenvironment that permits their development along multiple lineages at the expense of uni-lineage MF progenitors.

Recent work by the Rodewald's group suggested that fetal MFs arise from HSC-independent YS EMPs (Perdiguero et al., 2014); while we agree that EMPs arise in the YS and contribute to most tissue-resident MFs, our data clearly demonstrate that two waves of EMPs exist and differentially contribute to tissue MF populations. The primitive wave gives rise mostly to local YS MFs without monocytic intermediates, and then to microglia, and the definitive wave gives rise to FL MOs (among other lineages) which subsequently differentiate into tissue MFs. Our work emphasizes the necessary contribution of FL MOs to most tissue-resident MFs with the exception of microglia. Of note, in this prior study and as shown in our work, injection of 4'OHT at E8.5 or E9.5 in the inducible *Csf1r<sup>Cre/WT</sup>* model does not efficiently tag late EMPs and FL MOs, while efficiently labeling YS MFs. This is likely because early EMPs express CSF-1R mRNA, while late EMPs do not. Such differential expression of CSF-1R highlights the molecular heterogeneity of early versus late EMPs. Finally, absence of long-term follow up of the tagged cell progeny in the inducible *Csf1r<sup>Cre/WT</sup>* model limits the capacity to differentiate between the contribution of primitive versus definitive EMPs in this later study (Perdiguero et al., 2014).

The differences in EMP lineage potential could be acquired through expression of c-Myb, a transcription factor required for expansion and differentiation along each of the hematopoietic cell lineages (Ramsay and Gonda, 2008). C-Myb ablation compromises definitive hematopoiesis and leads to embryonic death at E15.5 (Mucenski et al., 1991): while the earliest YS progenitors, which give rise to microglia, do not express c-Myb (Kierdorf et al., 2013), we show that EMPs arising from E8.5 do. This agrees with previous reports indicating that primitive hematopoiesis can occur independently of c-Myb (Clarke et al., 2000), whereas EMPs from definitive hematopoiesis both express and depend upon c-Myb (Palis et al., 1999; Sumner et al., 2000; Yoder et al., 1997). Because fetal MOs are absent in c-Myb-deficient embryos (Mucenski et al., 1991; Schulz et al., 2012) and c-Myb expression is upregulated during fetal monopoiesis, it is likely that the change in EMP fate between the YS and the FL is orchestrated by c-Myb. Consequently, most tissue-resident MFs deriving from either HSC- dependent or independent fetal MOs, rely on c-Myb activity for their generation. Earlier findings in a different model suggested that tissue MFs derive from a c-Myb-independent lineage via YS MFs (Schulz et al., 2012). While embryonic YS MF numbers were unaffected by the absence of c-Myb, far fewer c-Kit<sup>+</sup> cells were present in the FL of *Myb<sup>-/-</sup>* embryos than wild-type (Schulz et al., 2012). Because our data suggest that EMPs express c-Myb in the YS and in the FL, whereas E10.5 YS MFs do not, we support the notion that late multipotent EMPs are Myb-dependent. As a result, their contribution to tissue-resident MF populations could not be evaluated in the *Myb<sup>-/-</sup>* embryos (Schulz et al., 2012). It may be that fetal MFs are unaffected in E16.5 *Myb<sup>-/-</sup>* embryos (Schulz et al., 2012) because they derive from c-Myb-independent early EMPs giving rise to primitive MFs able to occupy the empty niche left by the absence of c-Myb-dependent myeloid cells, as a compensatory mechanism.

Microglia have a unique origin, arising from YS MFs that maintain themselves by proliferating in situ throughout adulthood, and not from fetal MOs (Ginhoux et al., 2010; Kierdorf et al., 2013). The lack of contribution from MOs to the microglial progenitor pool could result either from a lack of intrinsic potential or a lack of access to the developing brain. The dual origin of LCs suggests that the progenitor differentiation program is not intrinsic to either YS- or FL-derived progenitors, but rather depends on tissue-specific extrinsic factors (Hoeffel et al., 2012). Corroborating the latter hypothesis, the blood-brain barrier is starting to be established around E13.5 (Daneman et al., 2010), precisely when fetal MOs colonize the tissues, thereby explaining the minor influx of fetal MOs to the embryonic brain. In addition, upon depletion of YS MFs, we observed the disappearance of microglial progenitors from E10.5 to E14.5, followed by a partial repopulation at E17.5 that will be completed after birth (Squarzoni et al., 2014), raising the question of the origin of the repopulating cells. The nature of the repopulating cell is under investigation, but we noted a major influx of MOs in the brain at E14.5, a population that is not found normally. In addition, preliminary data using our *S100a4*<sup>Cre/WT</sup> fate-mapping model combined with in utero depletion of YS MFs suggest that fetal MOs give rise to all repopulating fetal MF populations including microglia (data not shown), excluding the possibility that tissue MFs might formally be derived from YS MFs that escaped antibody depletion. This suggests that fetal MOs might give rise to microglia if they are able to access the brain rudiment (provided after YS MF depletion). Finally, these findings highlight the crucial role that tissues play in shaping the MF compartment, from the stage of controlling recruitment of MF progenitors right through until the maturation of recruited cells into the adult MF population.

Altogether our data provide a framework for the future investigation of adult MF population heterogeneity in both regard to their ontogeny, as well as their homeostasis at the progenitor level. This forms a firm grounding for our understanding of their roles in tissues in the steady state, as well as their involvement in diverse pathological settings and their potential as therapeutic targets including metabolic diseases, fibrosis, and carcinogenesis, and opens the door to MF-targeted therapeutic interventions.

## Experimental Procedures

### Cell Suspension Preparations

Mouse ears (split into dorsal and ventral parts) or whole skin (starting from E17.5) were first incubated for 2 hr in Hank's balanced salt solution (HBSS) containing Dispase (2.4 mg/ml, working activity of 1.7 U/mg; Invitrogen) to separate dermal and epidermal sheets before subsequent collagenase incubation. Whole tissues from adult mice, newborns or embryos were cut into small pieces, incubated in HBSS containing 10% fetal bovine serum and collagenase type IV (0.2 mg/ml, working activity of 770 U/mg; Sigma; 1 hr for adult tissues and newborns and 30 min for embryonic tissues) and then passaged through a 19G needle to obtain a homogeneous cell suspension. Embryonic blood cells were collected by decapitation in PBS 10 mM EDTA and red blood cells were lysed. When embryos were harvested prior to E13.5, the different tissues were isolated under a binocular microscope (Leica M320). For fetal liver cell suspensions, the whole liver was isolated and passed

through a 19G needle without collagenase treatment. Analysis was carried out by flow cytometry, gating on singlets of DAPI<sup>-</sup> (4,6-diamidino-2-phenylindole) CD45<sup>+</sup> cells.

### Induction of Cell Tagging with 4-Hydroxytamoxifen

For fate-mapping experiments, *Runx1*<sup>MerCreMer/WT</sup> × *Rosa*<sup>R26R-EYFP/R26R-EYFP</sup> mice were used as described (Samokhvalov et al., 2007). Briefly, 4-hydroxytamoxifen (4'OHT) (Sigma) was prepared as previously reported and administered by intraperitoneal injection (3–5 mg) to pregnant mice at 7.0–10.0 days post-conception (dpc). Day of embryonic development was estimated by taking the day of vaginal plug observation as 0.5 dpc. As 4'OHT treatment during pregnancy interferes with normal delivery, to trace cells marked during embryogenesis into adulthood, caesarean sections were carried out at term and neonates were fostered by lactating females. Active recombination in these genetically targeted mice occurs in a narrow time frame that does not exceed 24 hr post-injection and leads to irreversible expression of the enhanced yellow fluorescent protein (EYFP) in *Runx1*<sup>+</sup> cells and their progeny (Samokhvalov et al., 2007). Similar procedures were followed for the use of *Csf1r*<sup>MerCreMer/WT</sup> mice.

### Flow Cytometry

Flow cytometric studies were performed using a BD FACSCanto and a BD LSR II (BD Biosciences) with subsequent data analysis using FlowJo software (Tree Star). Fluorochrome- or biotin- conjugated monoclonal antibodies (mAbs) (see Supplemental Experimental Procedures), the corresponding isotype-matched controls, and secondary reagents were purchased either from BD Biosciences or eBioscience. Annexin-V staining was performed using the Annexin kit (BD PharMingen) according to the manufacturer's protocol.

### Yolk Sac Macrophage Depletion

Pregnant C57BL/6 females were treated with anti-CSF-1R mAb αCSF-1R, clone AFS98) or the rat IgG2a isotype control (clone R35-95; BD Biosciences) at E6.5 by intraperitoneal injection (3 mg, in sterile PBS). αCSF-1R mAb was purified from culture supernatant of AFS98 hybridoma (Sudo et al., 1995), grown in a CELLLine Flask (BD) in serum-free medium (PFHM-II; Invitrogen).

### In Vivo Proliferation Assay

Proliferation of monocyte and macrophage populations was investigated using the fluorescent ubiquitination-based cell-cycle indicator (Fucci) transgenic mouse model in which the green-emitting fluorescent protein Azami Green is fused to Geminin, a ubiquitination oscillator whose expression is regulated by cell-cycle-dependent proteolysis, resulting in the expression of fluorescence in cells in S/G2/M phases (Sakaue-Sawano et al., 2008) and their identification by flow cytometry.

## Statistical Analysis

Repeated-measures ANOVA, Mann-Whitney tests, and unpaired t tests (with a 95% confidence) were performed using Prism 6.0 (GraphPad Software). All p-values are two-tailed. \*p < 0.05; \*\*p < 0.01; and \*\*\*p < 0.001.

## Supplementary Material

Refer to Web version on PubMed Central for supplementary material.

## Acknowledgments

This work was supported by core grants of the Singapore Immunology Network to F.G., by NIH grants CA112100, HL086899, and AI080884 to M.M., by the NMRC Singapore (NMRC/CSA/012/2009) for J.K.Y.C. *Runt1-MerCreMer* mice have RIKEN CDB Acc. No. CDB0524K. We thank Dr. Lucy Robinson of Insight Editing London for her assistance in preparing the manuscript.

## References

- Bain CC, Bravo-Blas A, Scott CL, Gomez Perdiguero E, Geissmann F, Henri S, Malissen B, Osborne LC, Artis D, Mowat AM. Constant replenishment from circulating monocytes maintains the macrophage pool in the intestine of adult mice. *Nat Immunol.* 2014; 15:929–937. [PubMed: 25151491]
- Bertrand JY, Jalil A, Klaine M, Jung S, Cumano A, Godin I. Three pathways to mature macrophages in the early mouse yolk sac. *Blood.* 2005; 106:3004–3011. [PubMed: 16020514]
- Bhowmick NA, Chytil A, Plieth D, Gorska AE, Dumont N, Shappell S, Washington MK, Neilson EG, Moses HL. TGF-beta signaling in fibroblasts modulates the oncogenic potential of adjacent epithelia. *Science.* 2004; 303:848–851. [PubMed: 14764882]
- Böiers C, Carrelha J, Lutteropp M, Luc S, Green JC, Azzoni E, Woll PS, Mead AJ, Hultquist A, Swiers G, et al. Lymphomyeloid contribution of an immune-restricted progenitor emerging prior to definitive hematopoietic stem cells. *Cell Stem Cell.* 2013; 13:535–548. [PubMed: 24054998]
- Boyer SW, Schroeder AV, Smith-Berdan S, Forsberg EC. All hematopoietic cells develop from hematopoietic stem cells through Flk2/Flt3- positive progenitor cells. *Cell Stem Cell.* 2011; 9:64–73. [PubMed: 21726834]
- Buza-Vidas N, Woll P, Hultquist A, Duarte S, Lutteropp M, Bouriez-Jones T, Ferry H, Luc S, Jacobsen SE. FLT3 expression initiates in fully multipotent mouse hematopoietic progenitor cells. *Blood.* 2011; 118:1544–1548. [PubMed: 21628405]
- Christensen JL, Wright DE, Wagers AJ, Weissman IL. Circulation and chemotaxis of fetal hematopoietic stem cells. *PLoS Biol.* 2004; 2:E75. [PubMed: 15024423]
- Clarke D, Vegiopoulos A, Crawford A, Mucenski M, Bonifer C, Frampton J. In vitro differentiation of c-myb(-/-) ES cells reveals that the colony forming capacity of unilineage macrophage precursors and myeloid progenitor commitment are c-Myb independent. *Oncogene.* 2000; 19:3343–3351. [PubMed: 10918591]
- Cline MJ, Moore MA. Embryonic origin of the mouse macrophage. *Blood.* 1972; 39:842–849. [PubMed: 5028525]
- Daneman R, Zhou L, Kebede AA, Barres BA. Pericytes are required for blood-brain barrier integrity during embryogenesis. *Nature.* 2010; 468:562–566. [PubMed: 20944625]
- Dzierzak E, Speck NA. Of lineage and legacy: the development of mammalian hematopoietic stem cells. *Nat Immunol.* 2008; 9:129–136. [PubMed: 18204427]
- Epelman S, Lavine KJ, Beaudin AE, Sojka DK, Carrero JA, Calderon B, Brija T, Gautier EL, Ivanov S, Satpathy AT, et al. Embryonic and adult-derived resident cardiac macrophages are maintained through distinct mechanisms at steady state and during inflammation. *Immunity.* 2014; 40:91–104. [PubMed: 24439267]

- Frame JM, McGrath KE, Palis J. Erythro-myeloid progenitors: “definitive” hematopoiesis in the conceptus prior to the emergence of hematopoietic stem cells. *Blood Cells Mol Dis.* 2013; 51:220–225. [PubMed: 24095199]
- Friedman AD. Transcriptional regulation of granulocyte and monocyte development. *Oncogene.* 2002; 21:3377–3390. [PubMed: 12032776]
- Geissmann F, Jung S, Littman DR. Blood monocytes consist of two principal subsets with distinct migratory properties. *Immunity.* 2003; 19:71–82. [PubMed: 12871640]
- Ginhoux F, Jung S. Monocytes and macrophages: developmental pathways and tissue homeostasis. *Nat Rev Immunol.* 2014; 14:392–404. [PubMed: 24854589]
- Ginhoux F, Greter M, Leboeuf M, Nandi S, See P, Gokhan S, Mehler MF, Conway SJ, Ng LG, Stanley ER, et al. Fate mapping analysis reveals that adult microglia derive from primitive macrophages. *Science.* 2010; 330:841–845. [PubMed: 20966214]
- Golub R, Cumano A. Embryonic hematopoiesis. *Blood Cells Mol Dis.* 2013; 51:226–231. [PubMed: 24041595]
- Guilliams M, De Kleer I, Henri S, Post S, Vanhoutte L, De Prijck S, Deswarte K, Malissen B, Hammad H, Lambrecht BN. Alveolar macrophages develop from fetal monocytes that differentiate into long-lived cells in the first week of life via GM-CSF. *J Exp Med.* 2013; 210:1977–1992. [PubMed: 24043763]
- Hashimoto D, Chow A, Noizat C, Teo P, Beasley MB, Leboeuf M, Becker CD, See P, Price J, Lucas D, et al. Tissue-resident macrophages self-maintain locally throughout adult life with minimal contribution from circulating monocytes. *Immunity.* 2013; 38:792–804. [PubMed: 23601688]
- Hettinger J, Richards DM, Hansson J, Barra MM, Joschko AC, Krijgsveld J, Feuerer M. Origin of monocytes and macrophages in a committed progenitor. *Nat Immunol.* 2013; 14:821–830. [PubMed: 23812096]
- Hoeffel G, Wang Y, Greter M, See P, Teo P, Malleret B, Leboeuf M, Low D, Oller G, Almeida F, et al. Adult Langerhans cells derive predominantly from embryonic fetal liver monocytes with a minor contribution of yolk sac-derived macrophages. *J Exp Med.* 2012; 209:1167–1181. [PubMed: 22565823]
- Jakubzick C, Gautier EL, Gibbings SL, Sojka DK, Schlitzer A, Johnson TE, Ivanov S, Duan Q, Bala S, Condon T, et al. Minimal differentiation of classical monocytes as they survey steady-state tissues and transport antigen to lymph nodes. *Immunity.* 2013; 39:599–610. [PubMed: 24012416]
- Jenkins SJ, Ruckerl D, Cook PC, Jones LH, Finkelman FD, van Rooijen N, MacDonald AS, Allen JE. Local macrophage proliferation, rather than recruitment from the blood, is a signature of TH2 inflammation. *Science.* 2011; 332:1284–1288. [PubMed: 21566158]
- Kierdorf K, Erny D, Goldmann T, Sander V, Schulz C, Perdiguero EG, Wieghofer P, Heinrich A, Riemke P, Hölscher C, et al. Microglia emerge from erythromyeloid precursors via Pu.1- and Irf8-dependent pathways. *Nat Neurosci.* 2013; 16:273–280. [PubMed: 23334579]
- Kieusseian A, Brunet de la Grange P, Burlen-Defranoux O, Godin I, Cumano A. Immature hematopoietic stem cells undergo maturation in the fetal liver. *Development.* 2012; 139:3521–3530. [PubMed: 22899849]
- Kumaravelu P, Hook L, Morrison AM, Ure J, Zhao S, Zuyev S, Ansell J, Medvinsky A. Quantitative developmental anatomy of definitive haematopoietic stem cells/long-term repopulating units (HSC/RUs): role of the aorta-gonad-mesonephros (AGM) region and the yolk sac in colonisation of the mouse embryonic liver. *Development.* 2002; 129:4891–4899. [PubMed: 12397098]
- Lavin Y, Merad M. Macrophages: gatekeepers of tissue integrity. *Cancer immunology research.* 2013; 1:201–209. [PubMed: 24777851]
- Lin Y, Yoder MC, Yoshimoto M. Lymphoid progenitor emergence in the murine embryo and yolk sac precedes stem cell detection. *Stem Cells Dev.* 2014; 23:1168–1177. [PubMed: 24417306]
- Medvinsky A, Rybtsov S, Taoudi S. Embryonic origin of the adult hematopoietic system: advances and questions. *Development.* 2011; 138:1017–1031. [PubMed: 21343360]
- Molawi K, Sieweke MH. Transcriptional control of macrophage identity, self-renewal, and function. *Adv Immunol.* 2013; 120:269–300. [PubMed: 24070388]

- Moore MA, Metcalf D. Ontogeny of the haemopoietic system: yolk sac origin of in vivo and in vitro colony forming cells in the developing mouse embryo. *Br J Haematol.* 1970; 18:279–296. [PubMed: 5491581]
- Mucenski ML, McLain K, Kier AB, Swerdlow SH, Schreiner CM, Miller TA, Pietryga DW, Scott WJ Jr, Potter SS. A functional c-myb gene is required for normal murine fetal hepatic hematopoiesis. *Cell.* 1991; 65:677–689. [PubMed: 1709592]
- Naito M, Takahashi K, Nishikawa S. Development, differentiation, and maturation of macrophages in the fetal mouse liver. *J Leukoc Biol.* 1990; 48:27–37. [PubMed: 2358750]
- Orkin SH, Zon LI. Hematopoiesis: an evolving paradigm for stem cell biology. *Cell.* 2008; 132:631–644. [PubMed: 18295580]
- Palis J. Primitive and definitive erythropoiesis in mammals. *Frontiers in physiology.* 2014; 5:3. [PubMed: 24478716]
- Palis J, Yoder MC. Yolk-sac hematopoiesis: the first blood cells of mouse and man. *Exp Hematol.* 2001; 29:927–936. [PubMed: 11495698]
- Palis J, Robertson S, Kennedy M, Wall C, Keller G. Development of erythroid and myeloid progenitors in the yolk sac and embryo proper of the mouse. *Development.* 1999; 126:5073–5084. [PubMed: 10529424]
- Perdiguerro EG, Klapproth K, Schulz C, Busch K, Azzoni E, Crozet L, Garner H, Trouillet C, de Bruijn MF, Geissmann F, Rodewald HR. Tissue-resident macrophages originate from yolk-sac-derived erythro-myeloid progenitors. *Nature.* 2014; 518:547–551. [PubMed: 25470051]
- Qian BZ, Li J, Zhang H, Kitamura T, Zhang J, Campion LR, Kaiser EA, Snyder LA, Pollard JW. CCL2 recruits inflammatory monocytes to facilitate breast-tumour metastasis. *Nature.* 2011; 475:222–225. [PubMed: 21654748]
- Ramsay RG, Gonda TJ. MYB function in normal and cancer cells. *Nat Rev Cancer.* 2008; 8:523–534. [PubMed: 18574464]
- Sakaue-Sawano A, Kurokawa H, Morimura T, Hanyu A, Hama H, Osawa H, Kashiwagi S, Fukami K, Miyata T, Miyoshi H, et al. Visualizing spatiotemporal dynamics of multicellular cell-cycle progression. *Cell.* 2008; 132:487–498. [PubMed: 18267078]
- Samokhvalov IM, Samokhvalova NI, Nishikawa S. Cell tracing shows the contribution of the yolk sac to adult haematopoiesis. *Nature.* 2007; 446:1056–1061. [PubMed: 17377529]
- Schneider C, Nobs SP, Kurrer M, Rehrauer H, Thiele C, Kopf M. Induction of the nuclear receptor PPAR- $\gamma$  by the cytokine GM-CSF is critical for the differentiation of fetal monocytes into alveolar macrophages. *Nat Immunol.* 2014; 15:1026–1037. [PubMed: 25263125]
- Schulz C, Gomez Perdiguerro E, Chorro L, Szabo-Rogers H, Cagnard N, Kierdorf K, Prinz M, Wu B, Jacobsen SE, Pollard JW, et al. A lineage of myeloid cells independent of Myb and hematopoietic stem cells. *Science.* 2012; 336:86–90. [PubMed: 22442384]
- Serbina NV, Pamer EG. Monocyte emigration from bone marrow during bacterial infection requires signals mediated by chemokine receptor CCR2. *Nat Immunol.* 2006; 7:311–317. [PubMed: 16462739]
- Squarzoni P, Oller G, Hoeffel G, Pont-Lezica L, Rostaing P, Low D, Bessis A, Ginhoux F, Garel S. Microglia modulate wiring of the embryonic forebrain. *Cell Rep.* 2014; 8:1271–1279. [PubMed: 25159150]
- Sudo T, Nishikawa S, Ogawa M, Kataoka H, Ohno N, Izawa A, Hayashi S, Nishikawa S. Functional hierarchy of c-kit and c-fms in intramarrow production of CFU-M. *Oncogene.* 1995; 11:2469–2476. [PubMed: 8545103]
- Sumner R, Crawford A, Mucenski M, Frampton J. Initiation of adult myelopoiesis can occur in the absence of c-Myb whereas subsequent development is strictly dependent on the transcription factor. *Oncogene.* 2000; 19:3335–3342. [PubMed: 10918590]
- Takahashi K, Yamamura F, Naito M. Differentiation, maturation, and proliferation of macrophages in the mouse yolk sac: a light-microscopic, enzyme-cytochemical, immunohistochemical, and ultrastructural study. *J Leukoc Biol.* 1989; 45:87–96. [PubMed: 2536795]
- Tamoutounour S, Guillemins M, Montanana Sanchis F, Liu H, Terhorst D, Malosse C, Pollet E, Ardouin L, Luche H, Sanchez C, et al. Origins and functional specialization of macrophages and

of conventional and monocyte-derived dendritic cells in mouse skin. *Immunity*. 2013; 39:925–938. [PubMed: 24184057]

Tavian M, Péault B. Embryonic development of the human hematopoietic system. *Int J Dev Biol*. 2005; 49:243–250. [PubMed: 15906238]

van Furth R, Cohn ZA, Hirsch JG, Humphrey JH, Spector WG, Langevoort HL. The mononuclear phagocyte system: a new classification of macrophages, monocytes, and their precursor cells. *Bull World Health Organ*. 1972; 46:845–852. [PubMed: 4538544]

Yoder MC, Hiatt K, Dutt P, Mukherjee P, Bodine DM, Orlic D. Characterization of definitive lymphohematopoietic stem cells in the day 9 murine yolk sac. *Immunity*. 1997; 7:335–344. [PubMed: 9324354]

Yona S, Kim KW, Wolf Y, Mildner A, Varol D, Breker M, Strauss-Ayali D, Viukov S, Guillemins M, Misharin A, et al. Fate mapping reveals origins and dynamics of monocytes and tissue macrophages under homeostasis. *Immunity*. 2013; 38:79–91. [PubMed: 23273845]

**Highlights**

- Fetal tissue macrophages arise from two distinct developmental programs
- Early EMPs give rise to yolk sac macrophages without monocytic intermediates
- Late c-Myb<sup>+</sup> EMPs seed the fetal liver and give rise to fetal monocytes
- Fetal monocytes differentiate into macrophages able to self-renew into adulthood

**In Brief**

The identity of the embryonic precursors that give rise to adult tissue-resident macrophages is controversial. Here, Ginhoux and colleagues show that yolk sac macrophages are the main precursors of microglia, whereas most other macrophages derive from fetal monocytes that arise from late *c-myb*<sup>+</sup> erythro-myeloid progenitors generated in the yolk sac.

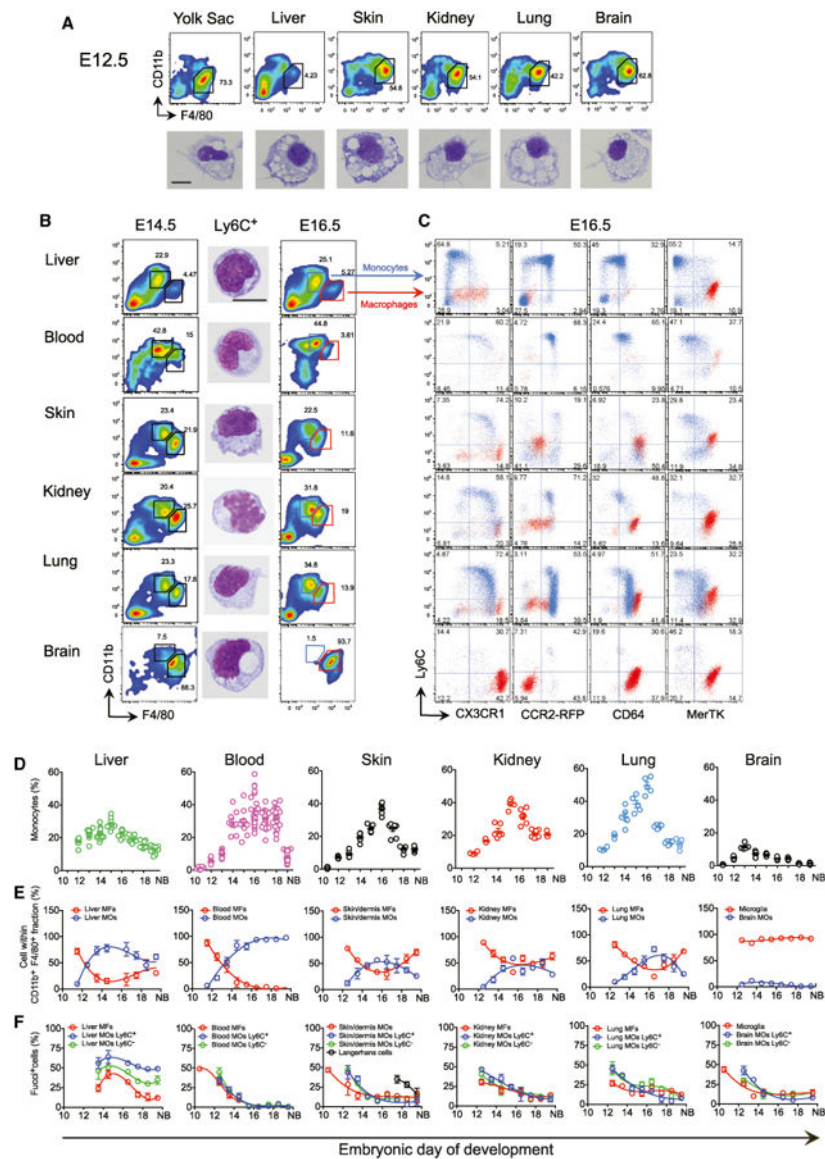


**Figure 1. Fetal Macrophages Arise Sequentially from YS Macrophages and Fetal Monocytes**  
 (A) Flow cytometry analysis of cells from E12.5 embryonic tissues and GIEMSA staining of purified doublet<sup>-</sup>DAPI<sup>-</sup>CD45<sup>+</sup>CD11b<sup>lo</sup>F4/80<sup>hi</sup>CD64<sup>+</sup>Ly6C<sup>-</sup>YS MFs from each tissue.

(B) Flow cytometry analysis of cells from E14.5 and E16.5 embryos and GIEMSA staining of purified doublet<sup>-</sup>DAPI<sup>-</sup>CD45<sup>+</sup>CD11b<sup>hi</sup>F4/80<sup>lo</sup>CD64<sup>+</sup>Ly6C<sup>+</sup> MOs from each E14.5 tissue. (A and B) Scale bar represents 5  $\mu$ M.

(C) Flow cytometry analysis of cells from E16.5 *Cx3cr1*<sup>+/gfp</sup>, *Ccr2*<sup>+/rfp</sup>, and WT embryos. Overlay of MFs (red population) and fetal MOs (blue population) is depicted (see also Figure S1A for FL analysis). Representative data from five embryos from two litters of each strain are shown.

(D) Kinetics of fetal MO tissue infiltration. Percentage of fetal CD11b<sup>hi</sup>F4/80<sup>lo</sup>CD64<sup>+</sup>Ly6C<sup>+/-</sup> MOs within doublet<sup>-</sup>DAPI<sup>-</sup>CD45<sup>+</sup> cells on alternate days

of embryonic development (see also Figure S1B for  $CCR2^{-/-}$  data). Each dot represents one embryo ( $n = 5-12$ ).

(E) MFs gated as in (A) and fetal MOs gated as in (B) within total  $CD11b^{+}F4/80^{+}$  cells ( $n = 5-12$ ).

(F) Percentage of proliferative MFs gated as in (A),  $Ly6C^{+}$  and  $Ly6C^{-}$  MOs gated as in (B) determined in Fucci reporter mice (see Supplemental Information,  $n = 5-8$ ) (see also Figure S2A for representative plots). Mean  $\pm$  SEM from three independent litters is presented in (D)–(F).

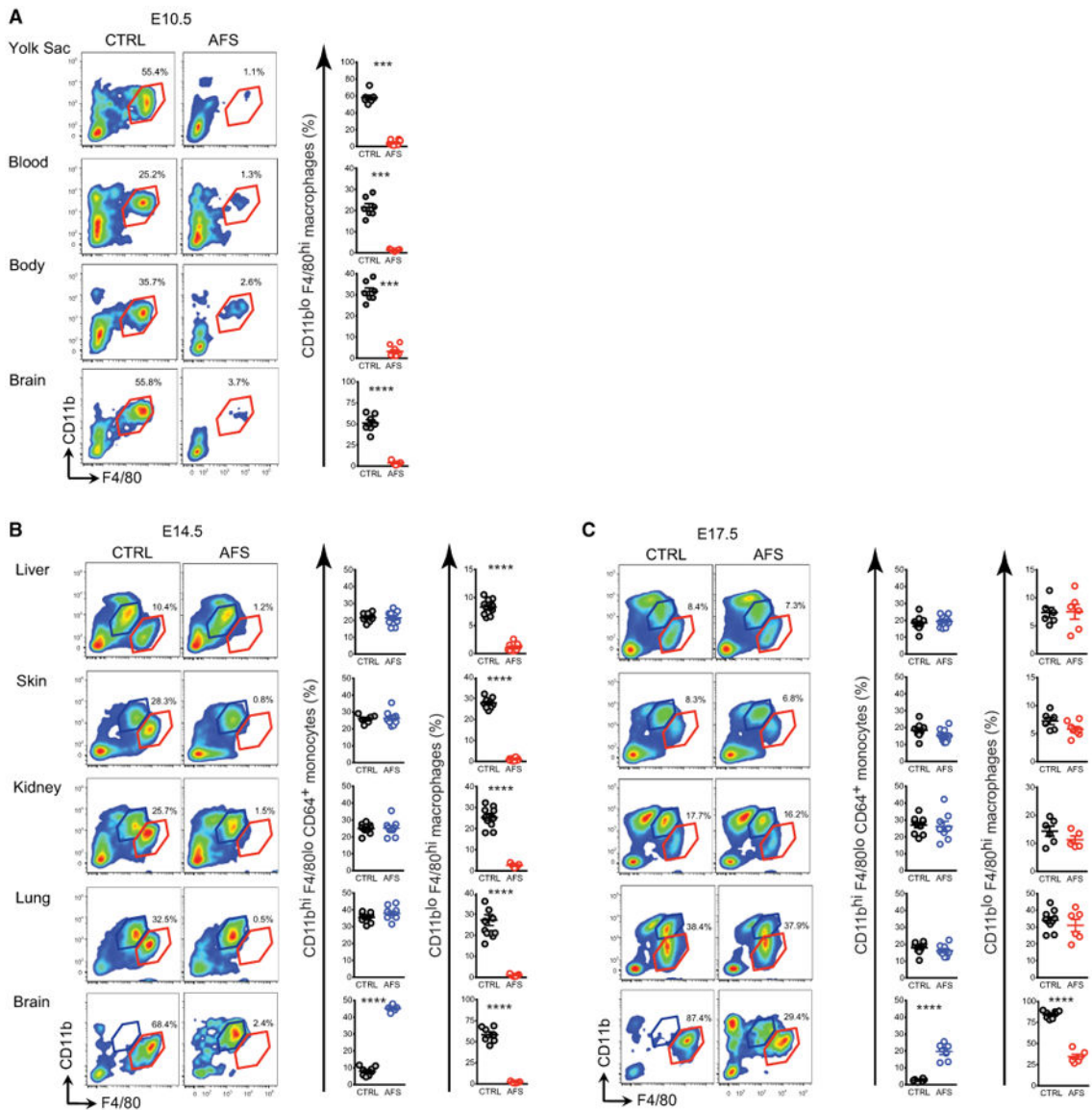


**Figure 2. YS Macrophages Are Not Essential for Fetal Macrophage Development**

(A–C) Pregnant females were untreated or injected with AFS98 at E6.5 and cells from embryos were analyzed by flow cytometry at E10.5 (A), E14.5 (B), and E17.5 (C).

Percentages of MFs (red) and fetal MOs (blue) gated as in Figure 1 are shown. Each dot represents one embryo. Bars represent mean ± SEM (\*p < 0.05; \*\*p < 0.01; \*\*\*p < 0.001; \*\*\*\*p < 0.0001). Analysis of n = 5–12 embryos per group from 2–3 independent litters (see also Figure S2B).

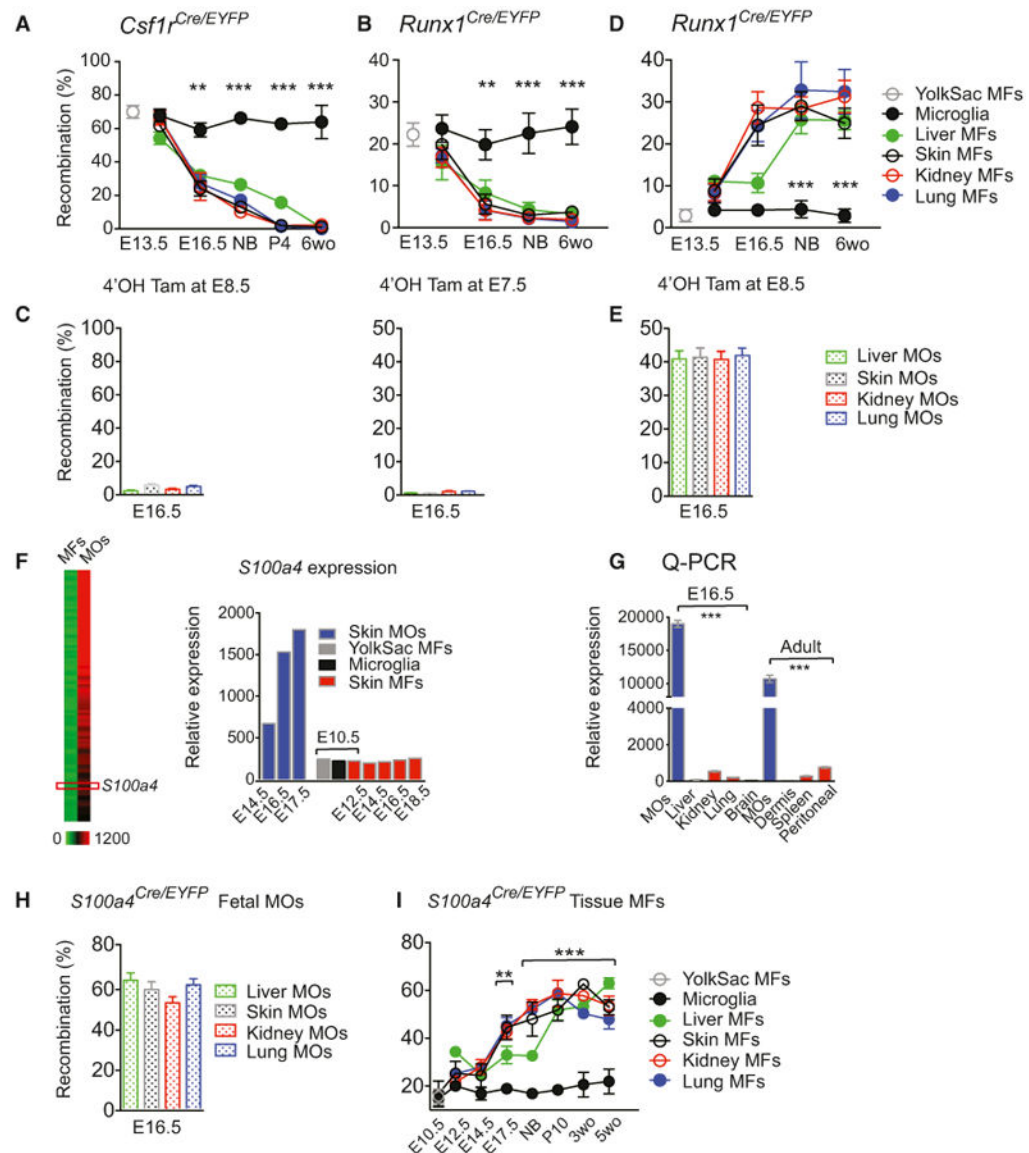


### Figure 3. YS Macrophages in Embryonic Tissues Are Progressively Replaced by Fetal Monocyte-Derived Macrophages

(A–E) Fate-mapping of YS MFs and fetal MOs from early development into adulthood (6 weeks old). Percentage of recombination in MFs at various time points (A), (B), and (D) or MOs at E16.5 (C) and (E) after a single injection of 4'OHT at E8.5 in *Csf1<sup>Cre</sup>/WT* pregnant mice (A, C, left) (two pooled experiments,  $n = 5–12$  for each time point), or at E7.5 (B, C, right) (three pooled experiments,  $n = 8–16$ , for each time point), or E8.5 (D) and (E) (two pooled experiments,  $n = 5–16$  for each time point) in *Runx1<sup>Cre</sup>/WT* pregnant mice.

(F) Heatmap depicting differentially expressed genes (DEG) in fetal MOs (See Supplemental Information and Figure S3A) and representative histograms of relative *S100a4* mRNA expression in MOs and MFs by gene array analysis. (G) *S100a4* mRNA expression determined by Q-PCR in MFs and fetal MOs ( $n = 3$ , each sample derives from at least eight embryos or five adult mice respectively). (H and I) Percentage of recombination in MOs at E16.5 (two pooled experiments,  $n = 5–10$ ) (H), and in MFs (two pooled

experiments, n = 5–10 for each time point) (I) of *S100a4*<sup>Cre/eyfp</sup> embryos and adult mice (see Figures S3B and S3C for controls). Bars represent mean  $\pm$  SEM (\*p < 0.05; \*\*p < 0.01; \*\*\*p < 0.001).

Author Manuscript

Author Manuscript

Author Manuscript

Author Manuscript

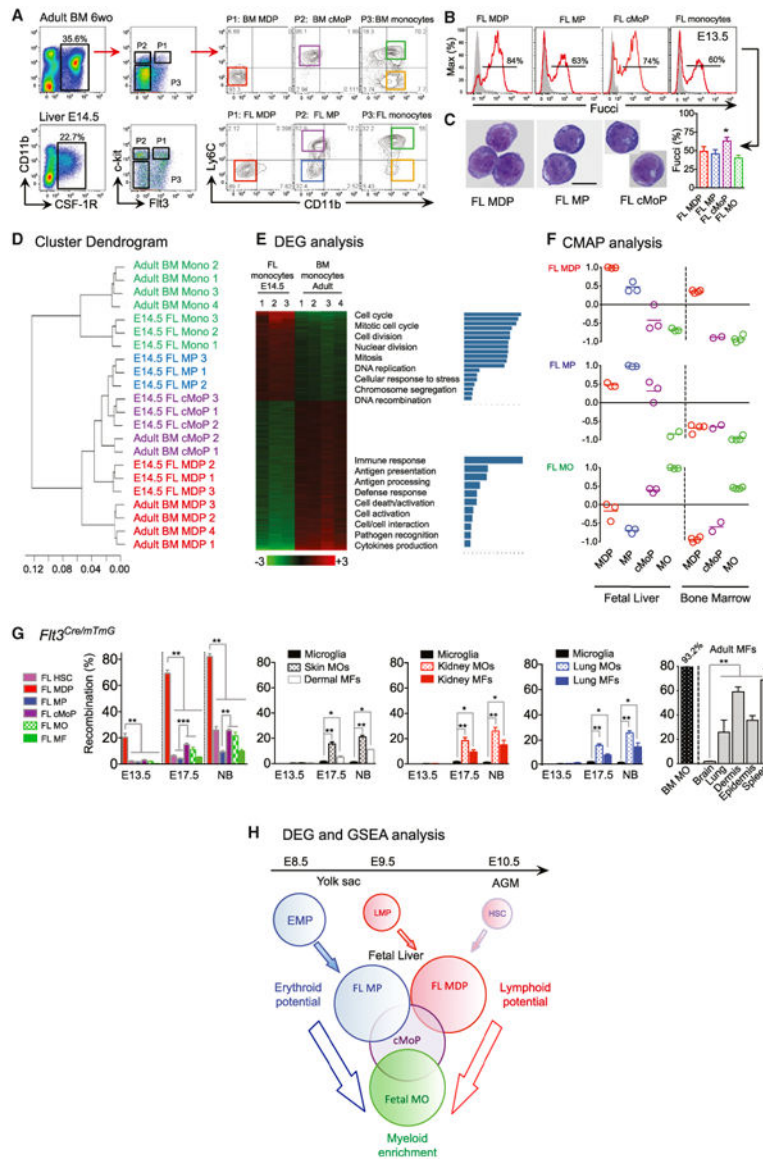


**Figure 4. Fetal Monocytes Arise from HSC-Independent and -Dependent Pathways**  
 (A) Gating strategy (from doublet<sup>-</sup>DAPI<sup>-</sup> cells) for myeloid progenitor identification in adult BM and E14.5 FL: MDP (Pt, then red gate), MP (P2, then blue gate), cMoP (P2, then purple gate), fetal Ly6C<sup>+</sup> MOs (P3, then green gate) and Ly6C<sup>-</sup> MOs (P3, then yellow gate) (see other time point and phenotype in Figures S4A and S4B).  
 (B and C) Proliferative activity analyzed in Fucci-reporter mice (n = 3–6) (B) and morphology visualized by GIEMSA staining of corresponding sorted FL myeloid progenitors (scale bar represents 5 μm; two independent experiments).  
 (D) Unsupervised clustering analysis of E14.5 FL and adult BM myeloid progenitors.  
 (E) Heatmap of DEG between FL and BM MOs with specific gene functionalities annotated.  
 (F) CMAP analysis identifies FL MDP and FL MP as early progenitors, and cMoP as an intermediate, in generating fetal MOs (See also Figures S4C–S4E, Supplemental Information and Table S1).  
 (G) Recombination percentages for *Fil3<sup>Cre/mTmG</sup>* in various tissues (Microglia, Skin MOs, Dermal MFs, Kidney MOs, Kidney MFs, Lung MOs, Lung MFs) at E13.5, E17.5, and NB. Significant recombination is observed in Microglia, Kidney MOs, and Lung MFs.  
 (H) Schematic of DEG and GSEA analysis showing the developmental trajectory from E8.5 (Yolk sac) to E9.5 (Fetal Liver) to E10.5 (AGM). Key populations include EMP, LMP, HSC, Fetal Liver (FL MP, FL MDP, cMoP), and Fetal MO (Myeloid enrichment).

(G) Percentage of recombination in  $Flt3^{Cre/mTmG}$  embryos/mice for FL MDP, FL MP, FL cMoP, FL MOs, or FL MFs (left), in MOs and MFs in skin, kidney and lung compared to microglia (middle) and in adult MOs and adult tissue MFs (right). Throughout the figure, bars represent mean  $\pm$  SEM (n = 3–6, two pooled experiments, \*p < 0.05; \*\*p < 0.01; \*\*\*p < 0.001).

(H) Scheme representing fetal monoipoiesis based on GSEA of each FL progenitor DEG combined with CMAP analysis (see also heatmap of FL myeloid progenitors DEG in Figure S4E, Tables S2 and S3 for GSEA details and Figure S4D for myeloid gene heatmap).

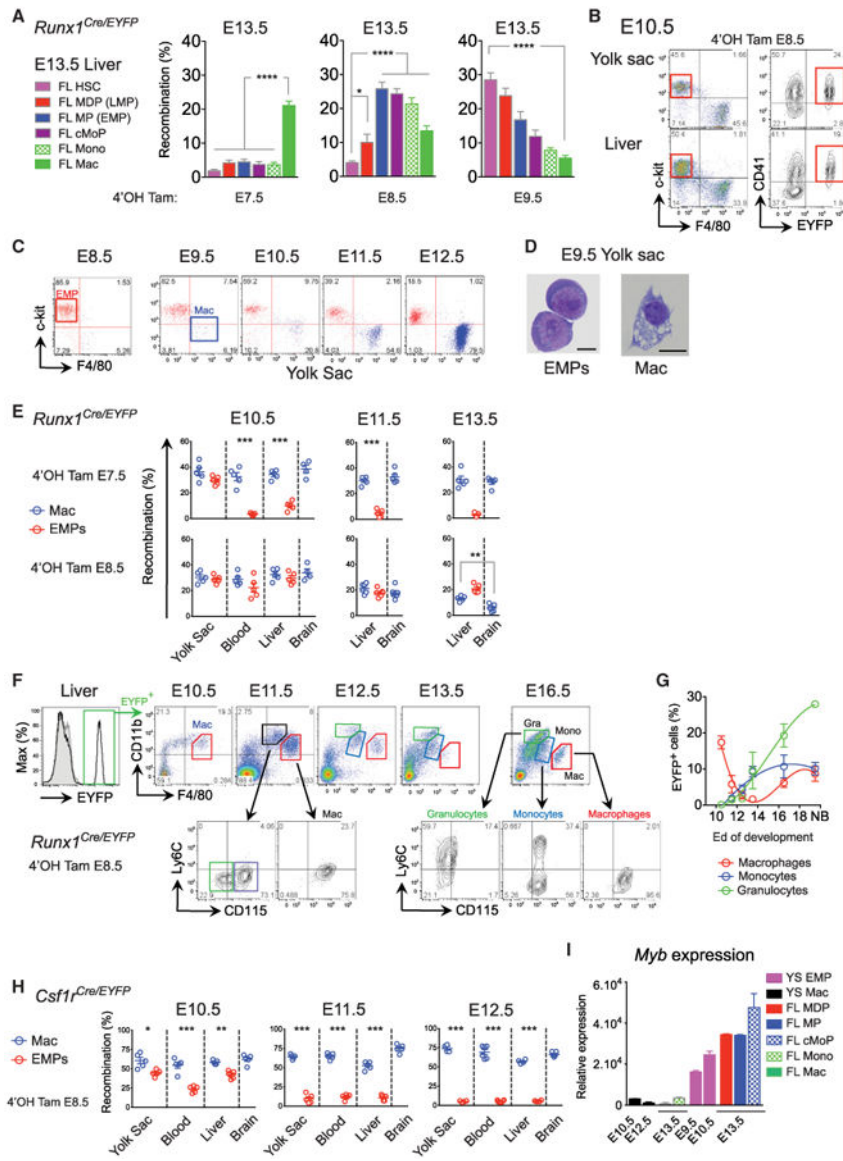


**Figure 5. *c-Myb*<sup>+</sup> EMPs Colonize the Fetal Liver and Give Rise to Monocytes**  
*Runx1*<sup>Cre/eyfp</sup> embryos activated either at E7.5, E8.5 or E9.5. Percentage of recombination in FL HSC, MDP, MP, cMoP, MOs, and MFs (two pooled litters, n = 7–13) (A) and in YS CD41<sup>+</sup> EMPs (B) (see also Figure S5 for gating strategy, pre-HSC, and EMP analysis). (C) The YS from E8.5 to E12.5 embryos were analyzed by flow cytometry for presence of c-Kit<sup>+</sup> progenitors and F4/80<sup>+</sup> MF. (D) E9.5 EMPs (doublet<sup>-</sup>DAPI<sup>-</sup>CD11b<sup>-</sup>F4/80<sup>-</sup>c-Kit<sup>+</sup>CD41<sup>+</sup>) and YS MFs (doublet<sup>-</sup>DAPI<sup>-</sup>CD11b<sup>+</sup>F4/80<sup>+</sup>) were sorted and visualized by GIEMSA staining. (E) *Runx1*<sup>Cre/eyfp</sup> embryos were activated at E7.5 (upper panels) or E8.5 (lower panels). Recombination profile in YS, blood and FL and brain MFs (blue) or EMPs (red) at E10.5, E11.5, and E13.5 are shown (n = 5–6 from two experiments). (F) Liver and Brain from E10.5, E11.5, E12.5, E13.5, and E16.5 embryos were analyzed by flow cytometry for presence of CD11b<sup>+</sup> and CD115<sup>+</sup> cells. (G) Percentage of EYFP<sup>+</sup> cells in Macrophages, Monocytes, and Granulocytes from E10.5 to E18.5. (H) *Csf1l1*<sup>Cre/eyfp</sup> embryos were activated at E10.5, E11.5, and E12.5. Recombination profile in YS, blood and FL and brain MFs (blue) or EMPs (red) at E10.5, E11.5, and E12.5 are shown (n = 5–6 from two experiments). (I) Relative *Myb* expression in YS EMP, YS Mac, FL MDP, FL MP, FL cMoP, FL Mono, and FL Mac at E10.5, E12.5, E13.5, and E13.5.

(F) EYFP<sup>+</sup> EMPs from *Runx1<sup>Cre/eyfp</sup>* activated at E8.5 and EMP progeny were followed in the FL during development. Primitive MFs (red), fetal MOs (blue), and granulocyte (green) generation is depicted.

(G) Quantification of MFs (red), fetal MOs (blue), and granulocytes (green) during development (n = 5–12 embryos from two independent experiments).

(H) *Csf1r<sup>Cre/eyfp</sup>* embryos were activated at E8.5. EYFP recombination at E10.5, E11.5, and E12.5 in YS, blood, FL and brain MFs (blue), or EMPs (red) are shown (n = 5–6 from two experiments).

(I) YS EMP, YS MF, FL myeloid progenitors, MOs, and MFs were sorted and c-Myb mRNA expression was measured by Q-PCR. Data are represented as mean ± SEM from triplicate samples where each sample was comprised of at least eight embryos. Throughout the figure, each dot represents one embryo; bars represent mean ± SEM (\*p < 0.05; \*\*p < 0.01; \*\*\*p < 0.001).